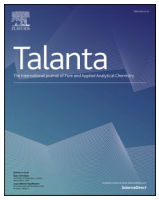
Talanta 292 (2025) 128010



Contents lists available at ScienceDirect

Talanta

journal homepage: www.elsevier.com/locate/talanta



A novel photosensitive nanoprobe combined with CRISPR/Cas12a for dual signal amplification detection of ANGPTL2

Xiuyu Chen [a,1], Dan Zhao [b,1], Changmin Yu [c], Jifu Wei [a,*], Guoren Zhou [a,**]

[a] Jiangsu Cancer Hospital, Jiangsu Institute of Cancer Research, The Affiliated Cancer, Hospital of Nanjing Medical University, Nanjing, 210009, Jiangsu, China
[b] School of Pharmacy, Nanjing University of Chinese Medicine, Nanjing, 210023, Jiangsu, China
[c] Key Laboratory of Flexible Electronics (KLOFE) and School of Flexible Electronics (Future Technologies), Nanjing Tech University (Nanjing Tech), Nanjing, 211800, China

ARTICLE INFO

Keywords:
CRISPR/Cas12a
Novel photosensitive nanoprobes
Signal amplification
Early diagnosis

ABSTRACT

The detection of specific protein biomarkers holds significant potential for the early diagnosis of colorectal cancer (CRC). However, the accurate quantification of low-abundance proteins in serum presents a major challenge due to factors such as limited sensitivity and the complexity of the required methodologies. In this work, we established a universal CRISPR/Cas biosensing platform by integrating novel photosensitive nanoprobes (DA/PL@Cu NPs) and CRISPR/Cas12 system (DPC-Cas) for the highly sensitive, specific and user-friendly detection of angiopoietin-like protein 2 (ANGPTL2). The DA/PL@Cu NPs serve as a critical component in the transduction of protein recognition information into nucleic acid amplification events to produce Cas12a activators. The DPC-Cas biosensor integrates DA/PL@Cu NPs-assisted amplification with Cas12a self-amplification, enabling ultrasensitive detection of ANGPTL2 at concentrations as low as 20.00 pg/mL. The proposed DPC-Cas biosensor successfully detected ANGPTL2 in serum, demonstrating significant potential for the early diagnosis of CRC.

1. Introduction

Colorectal cancer (CRC), the third most diagnosed cancer worldwide, poses a significant health threat and social burden [1,2]. The cure rate for early-stage CRC can exceed 90 %, while for advanced-stage CRC, it is less than 10 % [3,4]. Therefore, early diagnosis and treatment of CRC are critical strategies for reducing its mortality rate and improving patient outcomes. Currently, the gold standard for CRC screening remains colonoscopy [5,6]. However, patient compliance is often affected by the cumbersome bowel preparation process and the discomfort associated with this invasive procedure [7]. Non-invasive methods, such as fecal occult blood tests and fecal immunochemical tests, are the most widely used alternatives. However, their sensitivity for early-stage CRC diagnosis is relatively low, limiting their effectiveness [8,9]. As a result, the early diagnosis rate for CRC remains only 40 % [10]. Therefore, there is an urgent need for higher sensitivity and better specificity of non-invasive CRC diagnosis technology to improve the efficiency of diagnosis and the development of personalized medicine.

Liquid biopsy, which utilizes non-invasive samples such as blood or urine, has been recognized as a noninvasive, accessible, and real-time assessment method and represents a potential revolution in cancer diagnosis [11–13]. Currently, commonly used protein biomarkers for CRC include carcinoembryonic antigen and cancer antigen 19-9 [14,15]. However, these biomarkers have suboptimal sensitivity and specificity for early clinical diagnosis of CRC [16]. Therefore, the identification of more sensitive and specific CRC biomarkers is crucial to improving the early diagnostic rate of CRC.

Angiopoietin-like protein 2 (ANGPTL2) is a secreted protein belonging to the angiopoietin family. It serves as a pivotal mediator in chronic inflammation and metabolic dysregulation [17,18]. The upregulation of transcription factors in aggressive cancer cells promoted the increase of ANGPTL2 expression [19]. Most notably, cancer cell-derived ANGPTL2 increased the vitro motility and invasion in an autocrine/-paracrine manner, conferring an aggressive metastatic tumor phenotype [20]. High expression of ANGPTL2 in cancer cells inhibits anoikis and promotes ability of invasion, proliferation, migratory and is

* Corresponding author.
** Corresponding author.
E-mail addresses: weijifu@njmu.edu.cn (J. Wei), zhouguoren888@njmu.edu.cn (G. Zhou).
[1] Xiuyu Chen and Dan Zhao contributed equally to this work.

https://doi.org/10.1016/j.talanta.2025.128010
Received 7 February 2025; Received in revised form 20 March 2025; Accepted 22 March 2025
Available online 23 March 2025
0039-9140/© 2025 Elsevier B.V. All rights are reserved, including those for text and data mining, AI training, and similar technologies.

dramatically linked to cancer progression in patients with CRC [21]. Therefore, quantifying ANGPTL2 levels in serum may serve as an early indicator of potential tumorigenesis and holds significant clinical potential for the early diagnosis of CRC.

Currently, widely used methods for biomarker detection include enzyme-linked immunosorbent assay (ELISA) [22], mass spectrometry [23], and colorimetric sensing [24]. While these techniques are widely utilized due to their respective advantages, they still present several challenges. For example, ELISA involves a tedious detection procedure [25]. Mass spectrometry requires complex sample preparation and highly skilled operators [26], and colorimetric sensing is constrained by its relatively low sensitivity [27]. Therefore, there is an urgent need to develop more sensitive, efficient, and user-friendly clinical protein detection technologies.

The CRISPR/Cas system, particularly the Cas12a, exhibits excellent sensitivity, specificity as well as the high cleavage activity, showing great potential for biomarkers detection [27,28]. Cas12a′s collateral cleavage activity is triggered by target DNA recognition *via* CrRNA, leading to nonspecific degradation of fluorophore-quencher labeled nucleic acids [29–31]. This results in high turnover efficiency and significant self-signal amplification capability of the CRISPR/Cas12a system [32–34]. Although multiple turnovers have been achieved, the individual CRISPR/Cas12a method still insufficient for detecting lower concentrations of biomarkers in the early stage of cancer. Moreover, currently, CRISPR/Cas-based assays mainly focus on analyzing nucleic acid targets [35–37]. Therefore, it is still urgent to develop more sensitive CRISPR/Cas-based methods to meet the high demand of detecting ultralow abundance non-nucleic acid biomarkers in clinical applications. Nanoparticle-based amplification techniques, owing to their simple preparation, ease of modification and storage, high loading efficiency, and excellent biocompatibility, have found widespread application in biochemical detection, including functionalized copper nanoprobes (Cu NPs) [38–41]. The integration of nanoprobe technology with the CRISPR/Cas system presents a promising strategy for the ultrasensitive detection of non-nucleic acid targets.

Herein, we established the DPC-Cas biosensing platform for the highly sensitive, specific and user-friendly detection of ANGPTL2. The capture antibody-coated magnetic beads are employed to capture targets, and then the DA/PL@Cu NPs, loaded with detection antibodies (DA) and photosensitive linker probes (PL) are introduced to execute the sandwich-type recognition reaction. Upon detection, the signal of a single target is converted into numerous signals of PL through photolysis. Then, each of PL acts as the Cas12a activators for the *trans*-cleavage activity of Cas12a and releasing fluorescence. In this design, DA/PL@Cu NPs are crucial to transduce protein recognition information into nucleic acid amplification events, thus producing Cas12a activators. With dual cascade amplification including DA/PL@Cu NPs-assisted signal amplification and Cas12a self-signal amplification, even a small number of target molecules can generate intense fluorescence signals and enabling the ultrasensitive detection of trace target. The DPC-Cas biosensing platform holds tremendous potential in clinical diagnosis and enlarges the biosensor toolbox based on CRISPR/Cas technology for the analysis of non-nucleic acid targets.

2. Experimental section

2.1. Materials and reagents

PL, CrRNA, signal tag and magnetic beads were purchased from Sangon Inc. (Shanghai, China). Cu NPs was purchased from Hongwu International Co., Ltd. (Xuzhou, China). Cas12a and its reaction buffer were purchased from Kexin Biotechnology Co., Ltd. (Beijing, China). ANGPTL2 protein and its antibody were purchased from Abcam PIc. (Cambridge, UK). Tris (2-carboxyethyl) phosphine (TCEP) was purchased from Aladdin Biochemical Technology Co., Ltd. (Shanghai, China). Tris-HCl was purchased from Sinopharm Chemical Reagents, Co., Ltd. (Shanghai, China).

2.2. Instrumentation

The scanning electron microscope (SEM) images were taken on a Zeiss Sigma 500 (Carl Zeiss AG, Germany). The size and zeta potential of particles were taken on a Zs90 Zetasizer (Malvern, UK). Fourier transform infrared spectroscopy (FT-IR) spectroscopy was taken on an INVENIO-S FT-IR spectrometer (Bruker Corporation, Germany). Thermogravimetric (TGA) analysis was taken on a TGA2 TGA analyzer (Mettler Toledo, America). Polyacrylamide gel electrophoresis (PAGE) images were taken on a Tanon-4600SF gel imaging system (Tanon, China). Fluorescence intensity was measured by SpectraMax-iD5 fluorescence spectrophotometer (Molecular Devices, America). The DNA concentration was measured by a UV5Nano microvolume spectrophotometer (Mettler Toledo, America). The PL was photolyzed using a ZF-1A UV spectrophotometer (Qinke Analytical Instrument Co., Ltd., China).

2.3. Experimental methods

The detailed experimental methods are provided in Supplementary Information.

3. Results and discussion

3.1. Principle of ANGPTL2 detection based on DPC-Cas biosensor

The detection principle of the proposed DPC-Cas biosensor for dual signal amplification detection ANGPTL2 in serum was demonstrated in Fig. 1. Initially, capture antibody was immobilized on magnetic beads through a biotin-streptavidin interaction to enable specific recognition of the ANGPTL2 protein. Subsequently, a novel photosensitive DA/PL@Cu NPs was constructed by conjugating DA and PL to Cu NPs. Upon introduction of the target ANGPTL2, the DA/PL@Cu NPs bound to the capture antibody-functionalized magnetic beads, forming a sandwich complex. Afterwords, the PL was released from the complex *via* UV photolysis, converting the signal from a single target into a large number of PL molecules, thereby triggering the first stage of signal amplification. Finally, the released PL further activated Cas12a, resulting in the cleavage of multiple signal tags and triggering the second stage of signal amplification.

3.2. Preparation and characterization of the DA/PL@Cu NPs

First, thiol-modified PL, partially complementary to the CrRNA sequence, were conjugated to Cu NPs *via* Cu–S bonding to form PL@Cu NPs. The photosensitive group in PL was designed to release PL from the PL@Cu NPs upon UV exposure. After mixing with DA, the resulting encapsulated nanocomposite, DA/PL@Cu NPs, was obtained.

To obtain the optimal analytical performance, a series of experimental conditions were optimized. Theoretically, the higher the PL load, the greater the signal amplification. At a constant PL concentration, the mass of Cu NPs significantly influences the PL loading efficiency. The results indicated that when the mass of Cu NPs was 40 mg, only a trace amount of PL was detected in the supernatant of the reaction solution, suggesting that the PL modification on the Cu surface has effectively reached saturation (Fig. S1A). Furthermore, the reaction temperature and DA concentration were found to have a substantial impact on the detection performance. The optimal fluorescence intensity was observed at a reaction temperature of 25 °C (Fig. S1B) and a DA concentration of 3 μg (Fig. S1C). Finally, PL release was achieved by photolysis under the exposure of UV. Obviously, with the increase of the exposure time, the released amount of the PL increased gradually and achieved its highest value at 25 min (Fig. S1D).

Several methods were employed to characterize the newly

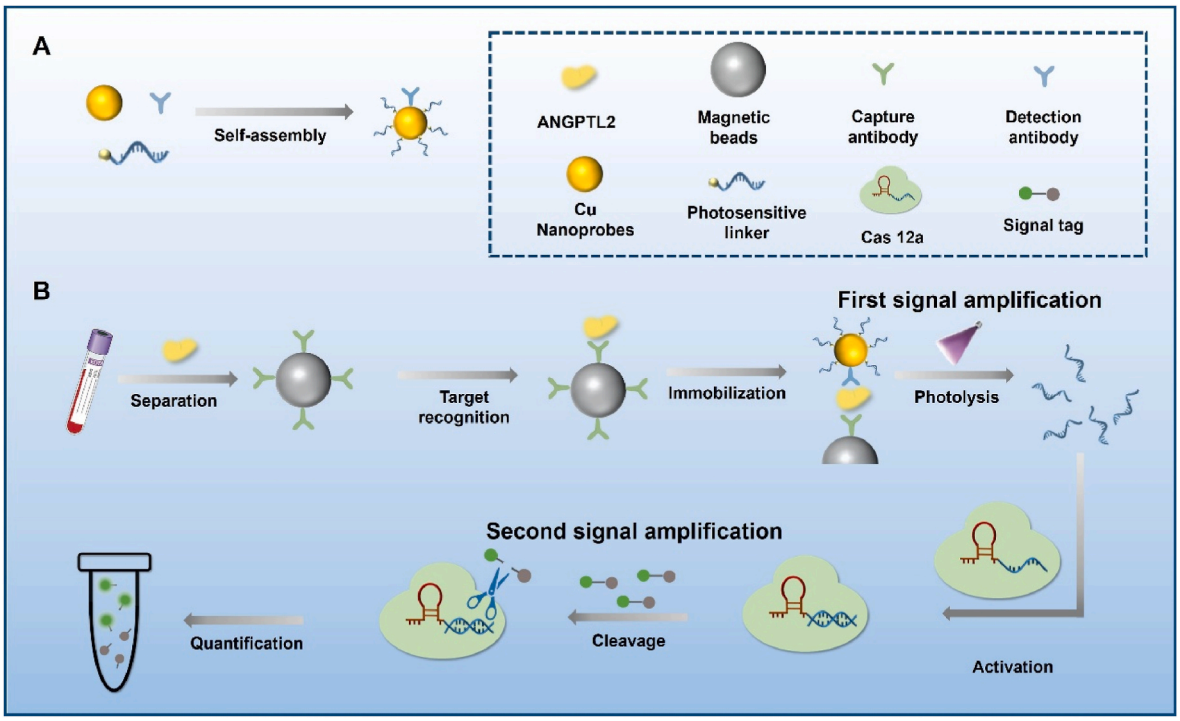


Fig. 1. Schematic illustration of the DPC-Cas biosensor for quantification of ANGPTL2 in serum. First, the ANGPTL2 protein was recognized by magnetic beads functionalized with capture antibody, forming a sandwich complex with DA/PL@Cu NPs. After magnetic separation, the DA/PL@Cu NPs were photolyzed, releasing a large amount of the PL and generating the first step of signal amplification. Finally, the released PL then activated Cas12a, which subsequently cleaved numerous signal tags, resulting in the second step of signal amplification.

synthesized DA/PL@Cu NPs. First, the results of SEM demonstrated the structure of the nanocomposites exhibited a regular spheroid (Fig. 2A–C). Furthermore, dynamic light scattering (DLS) results demonstrated that the average diameter of Cu NPs gradually increased from ~258 nm to ~313 nm with the sequential addition of the PL and DA (Fig. 2D). This result is consistent with the outcomes of SEM. Furthermore, the peak approximately 1200 cm^{-1} of PO_4^{3-} in the FT-IR spectrum of PL@Cu NPs, demonstrated the successful modification of PL (Fig. 2E). The signal at approximately 1600 cm^{-1} in the FT-IR spectra of the DA/PL@Cu NPs corresponded to the C═O stretching mode of the DA. In the TGA, a weight loss of 9.89 % between 240 °C and 420 °C can be attributed to the PL (Fig. 2F). In addition, the zeta potential of PL@Cu NPs was in a negative state, in contrast to that of Cu NPs, further confirming the successful modification with PL (Fig. S2).

3.3. Feasibility and optimization of CRISPR/Cas12a-based fluorescence detection system

Firstly, the feasibility study of CRISPR/Cas12a collateral cleavage was investigated under different reaction components for PL analysis.

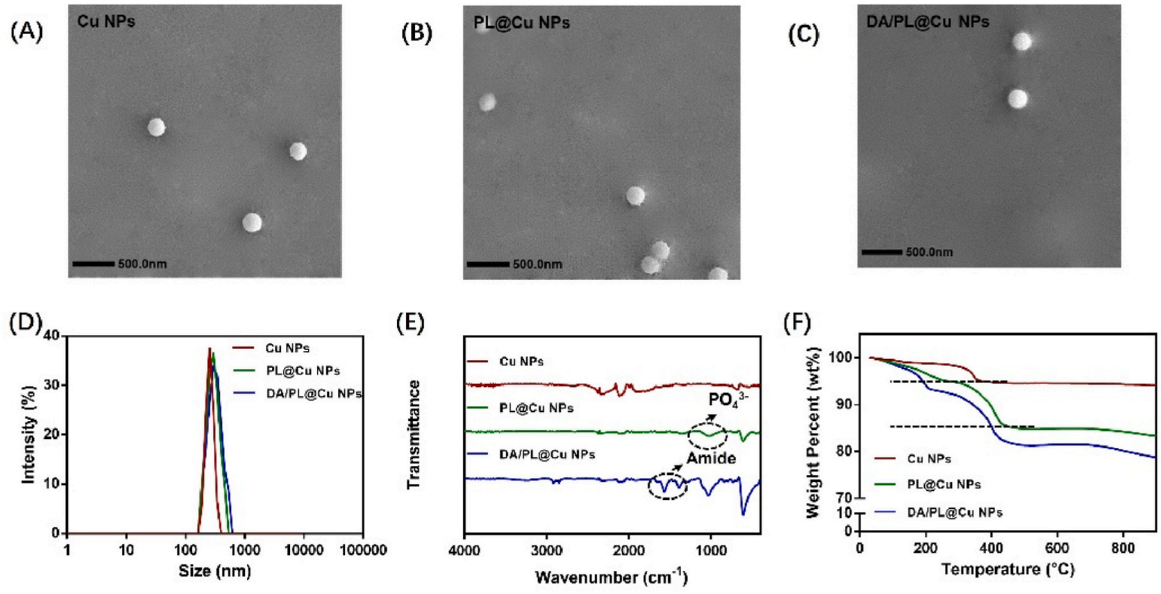


Fig. 2. Characterization of the DA/PL@Cu NPs using (A–C) SEM, (D) DLS, (E), FT-IR and (F) TGA.

The FAM-labeled signal tags are high-efficiently cleaved to produce an intense fluorescence signal (red line) only by combining the Cas12a, CrRNA, and PL (Fig. 3A). In contrast, the fluorescence response is negligible in the absence of either Cas12a, CrRNA, or PL. Subsequently, the fluorescence kinetic curves were also recorded to test the feasibility of CRISPR/Cas12a responses. Compared with the control group, a significantly enhanced fluorescence signal could be observed in the existence of 10 nM PL (Fig. 3B).

To achieve the best sensitivity performance, the optimized conditions for *trans*-cleavage activity were evaluated. Since the length of the PL sequence affects the cleavage efficiency of Cas12a, the length of PL was evaluated in this study. First, PAGE was performed to certify the reaction process. When the PL length was 22 bp, it could stably hybridize with the CrRNA (Fig. S3A). The fluorescence intensity increased with the increasing length of PL in the range of 22 bp-28 bp (Fig. S3B). When the length of PL was higher than 28 bp, the fluorescence intensity did not increase significantly. Therefore, we selected a PL length of 28 bp and the corresponding CrRNA as the final sequence. The specific sequence is provided in Table S1, and the secondary structure of PL-28 and CrRNA-28 are shown in Fig. S4.

The reaction time found to have a substantial impact on the cleavage efficiency of Cas12a. The cleavage speeds of Cas12a activated by enzymatic product in different time intervals indicates a minimum time of 30 min required to reach the equilibrium (Fig. S5A). Hence, 30 min was found to be best reaction time for Cas12a reacted with CrRNA. Then, the reaction temperature also greatly affects the cleavage efficiency of Cas12a. The reaction temperature of 25, 31, 37 and 43 °C were evaluated in this study (Fig. S5B). When the reaction temperature was on 37 °C, the highest fluorescence intensity was reached. Hence, the reaction temperature of 37 °C was selected for use in the following experiments. Furthermore, the *trans*-cleavage performance in different concentrations of signal tag cleavage substrates ranging from 250 to 1000 nM was evaluated (Fig. S5C). The fluorescence intensity generated by *trans*-cleavage was found to be directly proportional to the substrate concentration. These results aligned with the kinetics of enzyme-catalyzed reactions and followed the Michaelis-Menten equation when the signal tag concentration ranged from 250 to 750 nM. However, the cleavage rate decreased as the concentration of the signal tag increased beyond this range. This decrease may be attributed to the limitations of using fluorescence generation rates to calculate the cleavage rate. To establish a direct relationship between target concentration and fluorescence growth rate, a signal tag concentration of 750 nM was selected for the experiment. Moreover, efficient Cas12a/CrRNA duplex concentration plays an important role in achieving satisfactory performance. We further investigated the ratio of Cas12a to CrRNA ranging from 10:1 to 1:10 (Fig. S5D). Hence, owing to the highest fluorescence signal intensity, the Cas12a/CrRNA ratio of 1:1 (100 nM:100 nM) was selected for use in the following experiments. What is more, Cas12a showed different *trans*-cleavage activities in PBS, Tris-HCl and Cas reaction buffer (Fig. S5E). This may result from different concentrations of anions and cations. Hence, owing to the highest fluorescence signal intensity, the Cas reaction buffer was selected as an optimized buffer for further experiments. In addition, RNase effects CrRNA mediated CRISPR/Cas12a cleavage efficiency, especially in human plasma. The addition of RNase inhibitor produced an increase of fluorescence signal in comparison with no RNase inhibitor, indicating an effective inhibition of RNase (Fig. S5F).

Furthermore, the impact of different Cas12a sources on signal amplification was systematically evaluated, including LbCas12a from *Lachnospiraceae bacterium*, AsCas12a from *Acidaminococcus* sp., and ArCas12a from *Agathobacter rectalis* bacterium. Among them, LbCas12a exhibited the highest fluorescence signal intensity compared to AsCas12a and ArCas12a, indicating its superior performance in signal amplification (Fig. S6). Based on these results, LbCas12a was selected for further use in subsequent experiments to ensure optimal assay sensitivity and efficiency.

3.4. Analytical performance of DPC-Cas biosensor for detection of ANGPTL2

Under optimal conditions, we explore the performance of the DPC-Cas biosensor by detecting ANGPTL2. As depicted in Fig. 4A, the fluorescence intensity progressively ascends with the ANGPTL2 dosage raising from 10.00 to 500.0 pg/mL. The signal-to-noise (S/N) ratios for ANGPTL2 at concentrations of 10.00, 20.00, 50.00, 100.0, and 500.0 pg/mL were 2, 3, 10, 16, and 21, respectively. The limit of detection (LOD) for ANGPTL2 was determined to be 20.00 pg/mL (S/N = 3), while the limit of quantification (LOQ) was established at 50.00 pg/mL (S/N = 10). The performance of the prepared DPC-Cas biosensor was compared with existing detection methods, such as ELISA, mass spectrometry, and colorimetric sensing (Table S2). The DPC-Cas biosensor demonstrated a lower LOD than these conventional methods, highlighting its superior sensitivity. Additionally, the DPC-Cas biosensor required significantly less detection time compared to both ELISA and mass spectrometry, making it more time-efficient for practical applications. These advantages, combined with the operational convenience of the DPC-Cas platform, establish it as a highly promising method for biomarker detection.

Furthermore, some interferential proteins, such as bovine serum albumin, immunoglobulin G, cancer antigen 19-9, alpha-fetoprotein and their mixtures were also analyzed by use of ANGPTL2-specific magnetic beads to assess the selectivity of the proposed DPC-Cas biosensor (Fig. 4B). It can be seen that only ANGPTL2 can produce a remarkable fluorescence response, while the fluorescence responses generated by interferential proteins are all negligible and similar to that of blank control. Additionally, the detection performance of the proposed DPC-

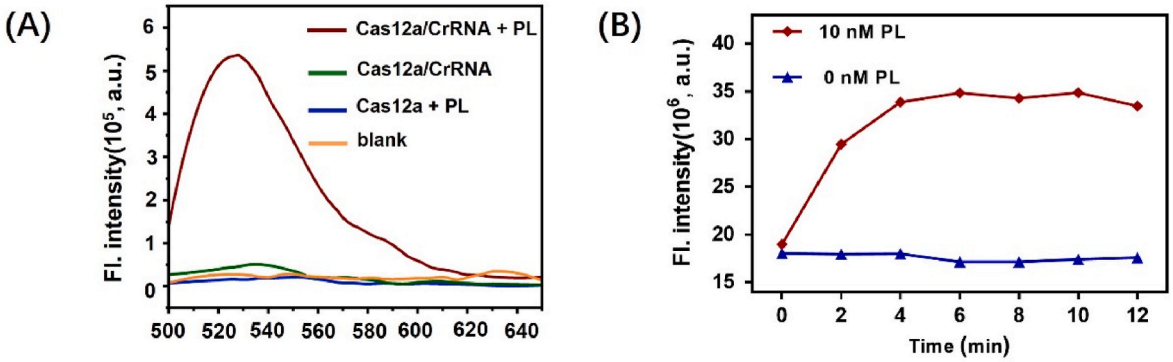


Fig. 3. Validation the feasibility of CRISPR/Cas12a-based fluorescence detection system. (A) Fluorescence spectra of CRISPR/Cas12a-based fluorescence detection system for the detection of 10 nM PL under different reaction components. (B) The fluorescence kinetic curves CRISPR/Cas12a-based fluorescence detection system.

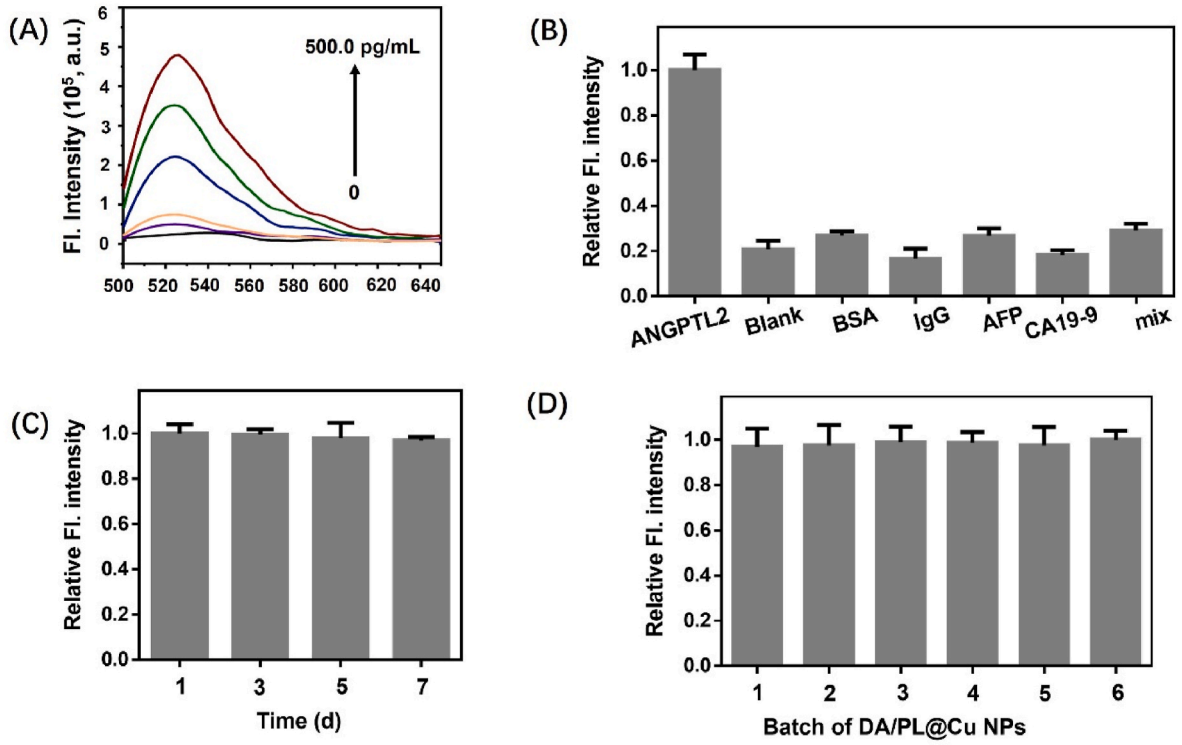


Fig. 4. Validation of the DPC-Cas biosensor for detection of ANGPTL2. (A) Fluorescence spectra of the approach for detection of ANGPTL2 at different concentrations (Blank, 10.00, 20.00, 50.00, 100.0 and 500.0 pg/mL). (B) The fluorescence signals detected using different targets, including ANGPTL2, bovine serum albumin (BSA), immunoglobulin G (IgG), cancer antigen 19-9 (CA19-9), alpha-fetoprotein (AFP) and their mixtures (mix). (C) The fluorescence signals detected using the DA/PL@Cu NPs through a week. (D) The fluorescence signals detected using six different batches of DA/PL@Cu NPs. Error bars represent the standard deviations of three replicate measurements.

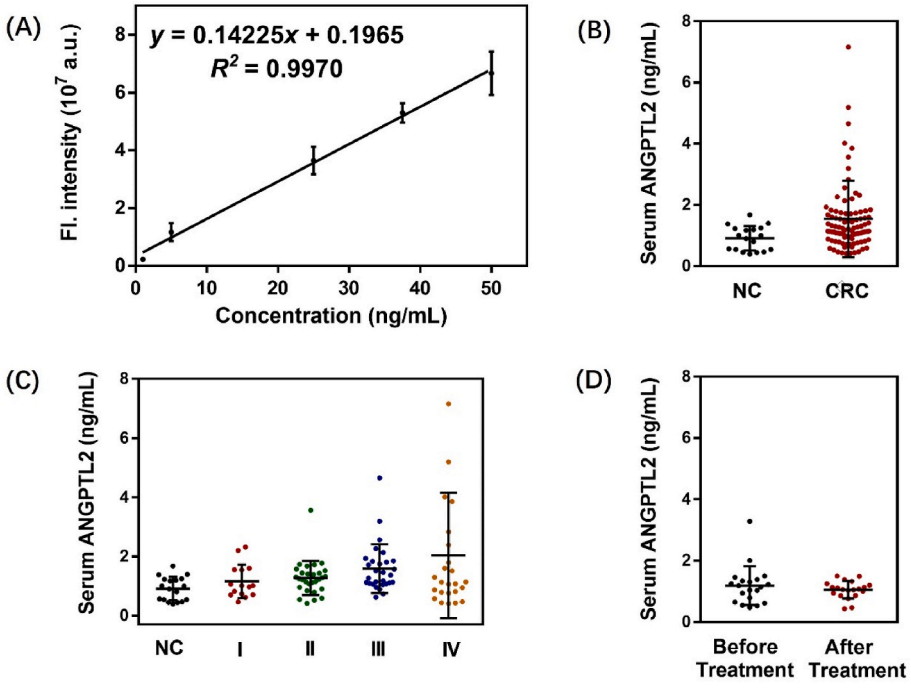


Fig. 5. Detection of ANGPTL2 using DPC-Cas biosensor. (A) Standard curve correlating fluorescence signals with ANGPTL2 concentration. (B) Detection of ANGPTL2 in the serum of normal controls (NC) (n = 18) and colorectal cancer (CRC) patients (n = 98). (C) Detection of ANGPTL2 in the serum of NC and CRC patients at different disease stages. (D) Detection of ANGPTL2 in the serum of CRC patients before and after treatment (n = 20). Error bars represent the standard deviations of three replicate measurements.

Cas biosensor was systematically evaluated in various serum matrices, including serum from healthy individuals and patients with CRC, breast cancer, lung cancer and gastric cancer. To assess the matrix effect, the ANGPTL2 standard was dissolved in PBS as well as different types of diluted serum, and the detection signals remained consistent across all conditions (Fig. S7). The coefficient of variation (CV) was calculated to be 4.08 %, demonstrating the robustness and broad applicability of the proposed biosensor for reliable detection in complex biological samples.

Moreover, to assess the stability of DA/PL@Cu NPs in ANGPTL2 detection, fluorescence signals were monitored at different time points over a one-week storage period. The results indicated excellent stability, with the fluorescence signal maintaining 96.89 % of its initial intensity after seven days of storage (Fig. 4C). These findings confirm the robustness and reproducibility of the nanoprobes, underscoring their potential for long-term and reliable biosensing applications. Additionally, to comprehensively evaluate the reproducibility of the proposed approach, we synthesized and analyzed six independent batches of DA/PL@Cu NPs. The CV among these batches was determined to be 1.19 %, demonstrating high consistency in the synthesis process and minimal batch-to-batch variation, thereby ensuring the reliability of the DPC-Cas biosensor (Fig. 4D). Finally, the detection of spiked recovery was carried out at different concentrations of ANGPTL2. The results showed good consistency between the detected concentrations and the spiked concentrations, with a recovery rate ranging from 98.35 % to 109.3 % (Table S3).

After validation of the DPC-Cas strategy, a concentration range of 1.000–50.00 ng/mL was obtained, and the regression equation was expressed as $y = 0.14225x+0.1965$, with a coefficient of determination (R^2) was 0.9970 (Fig. 5A). Then, the proposed assay was successfully employed to detect serum ANGPTL2 levels in a subset of 98 CRC patients and 18 normal controls (NC) (Table S4). In comparison to NC, serum levels of ANGPTL2 were significantly higher in CRC patients ($P < 0.05$) (Fig. 5B). Moreover, significantly higher ANGPTL2 levels were observed in stage I and II CRC patients compared to NC ($P < 0.05$), which reveals that ANGPTL2 could be used as a potential diagnostic biomarker for the identification of early CRC patients (Fig. 5C). Additionally, serum ANGPTL2 levels also found increased with TNM stage, which reveals that ANGPTL2 may be involved in the progression of CRC (Fig. 5C). Finally, serum ANGPTL2 levels were also quantified before and after treatment of CRC patients. Serum ANGPTL2 levels were found decreased after treatment of CRC patients, however, no significant differences were observed for discriminating CRC patients before and after treatment (Fig. 5D).

4. Conclusion

In summary, we developed a DPC-Cas biosensing strategy by integrating dual-functionalized DA/PL@Cu NPs with the CRISPR/Cas12a system for the highly sensitive, specific and user-friendly detection of ANGPTL2 in serum. Leveraging dual signal amplification, the proposed biosensor achieved an ultrasensitive detection limit of 20.00 pg/mL. Notably, this strategy exhibited excellent analytical performance in distinguishing CRC patients from NC, highlighting its potential for clinical diagnostics. Moreover, by modifying the recognition elements on magnetic beads and DA/PL@Cu NPs, this method can be adapted for the detection of other protein biomarkers. In future work, we will focus on designing novel recognition elements and nanoprobes with enhanced performance to further improve the robustness of this method.

CRediT authorship contribution statement

Xiuyu Chen: Writing – review & editing, Writing – original draft, Validation, Methodology, Investigation, Data curation, Conceptualization. **Dan Zhao:** Writing – review & editing, Writing – original draft, Validation, Methodology, Investigation, Data curation, Conceptualization. **Changmin Yu:** Writing – review & editing, Validation, Methodology, Investigation, Data curation. **Jifu Wei:** Writing – review & editing, Supervision, Project administration, Funding acquisition, Conceptualization. **Guoren Zhou:** Writing – review & editing, Supervision, Project administration, Funding acquisition, Conceptualization.

Declaration of competing interest

The authors declare that they have no known competing financial interests or personal relationships that could have appeared to influence the work reported in this paper.

Acknowledgements

This work was supported by the Nanjing Municipal Science and Technology Bureau (No. 202305027), Yishan Research Project of Jiangsu Cancer Hospital (No. YSZD202409 and YSZD202406), and Research Project of Jiangsu Cancer Hospital (No. QZLC202413).

Appendix A. Supplementary data

Supplementary data to this article can be found online at https://doi.org/10.1016/j.talanta.2025.128010.

Data availability

Data will be made available on request.

References

[1] R.L. Siegel, A.N. Giaquinto, A. Jemal, Cancer statistics, 2024, CA Cancer J. Clin. 74 (1) (2024) 12–49, https://doi.org/10.3322/caac.21820.
[2] N. Keum, E. Giovannucci, Global burden of colorectal cancer: emerging trends, risk factors and prevention strategies, Nat. Rev. Gastroenterol. Hepatol. 16 (12) (2019) 713–732, https://doi.org/10.1038/s41575-019-0189-8.
[3] Y. Cao, N. Wang, X. Wu, W. Tang, H. Bao, C. Si, P. Shao, D. Li, X. Zhou, D. Zhu, S. Yang, F. Wang, G. Su, K. Wang, Q. Wang, Y. Zhang, Q. Wang, D. Yu, Q. Jiang, J. Bao, L. Yang, Multidimensional fragmentomics enables early and accurate detection of colorectal cancer, Cancer Res. 84 (19) (2024) 3286–3295, https://doi.org/10.1158/0008-5472.CAN-23-3486.
[4] D.A. Corley, T.R. Levin, C.A. Doubeni, Adenoma detection rate and risk of colorectal cancer and death, N. Engl. J. Med. 370 (26) (2014) 2541, https://doi.org/10.1056/NEJMoa1309086.
[5] F.E. Juul, A.J. Cross, R.E. Schoen, C. Senore, P.F. Pinsky, E.A. Miller, N. Segnan, K. Wooldrage, P. Wieszczy-Szczepanik, P. Armaroli, K.K. Garborg, H.O. Adami, G. Hoff, M. Kalager, M. Bretthauer Øyvind Holme, M. Løberg, Effectiveness of colonoscopy screening vs sigmoidoscopy screening in colorectal cancer, JAMA Netw. Open 7 (2) (2024) e240007, https://doi.org/10.1001/jamanetworkopen.2024.0007.
[6] P.H.A. Wisse, S.Y. de Boer, M. Oudkerk Pool, J.S. Terhaar Sive Droste, C. Verveer, G.A. Meijer, E. Dekker, M.C.W. Spaander, Post-colonoscopy colorectal cancers in a national fecal immunochemical test-based colorectal cancer screening program, Endoscopy 56 (5) (2024) 364–372, https://doi.org/10.1055/a-2230-5563.
[7] L. Zhen, X. Tang, Z. Xu, Y. Huang, X. Qian, H. Lin, C. Li, R. Cui, H. Fang, H. Yang, J. Qiu, Z. Fang, X. Peng, Y. Jin, J. Nie, S. Guo, Y. Wang, M. Zhong, H. Gu, H. Xu, Early diagnosis of colorectal cancer based on bisulfite-free site-specific methylation identification PCR strategy: high-sensitivity, accuracy, and primary medical accessibility, Adv. Sci. 11 (33) (2024) e2401137, https://doi.org/10.1002/advs.202401137.
[8] F.A. Sinicrope, Increasing incidence of early-onset colorectal cancer, N. Engl. J. Med. 386 (16) (2022) 1547–1558, https://doi.org/10.1056/NEJMra2200869.
[9] A. Shaukat, T.R. Levin, Current and future colorectal cancer screening strategies, Nat. Rev. Gastroenterol. Hepatol. 19 (8) (2022) 521–531, https://doi.org/10.1038/s41575-022-00612-y.
[10] E.K. Barnell, E.M. Wurtzler, J. La Rocca, T. Fitzgerald, J. Petrone, Y. Hao, Y. Kang, F.L. Holmes, D.A. Lieberman, Multitarget stool RNA test for colorectal cancer screening, JAMA 330 (18) (2023) 1760–1768, https://doi.org/10.1001/jama.2023.22231.
[11] P. Pisapia, J.L. Costa, F. Pepe, G. Russo, G. Gragnano, A. Russo, A. Iaccarino, D. de Miguel-Perez, M.J. Serrano, V. Denninghoff, L. Quagliata, C. Rolfo, U. Malapelle, Next generation sequencing for liquid biopsy based testing in non-small cell lung cancer in 2021, Crit. Rev. Oncol. Hematol. 161 (2021) 103311, https://doi.org/10.1016/j.critrevonc.2021.103311.
[12] L. Chang, J. Li, R. Zhang, Liquid biopsy for early diagnosis of non-small cell lung carcinoma: recent research and detection technologies, Biochim. Biophys. Acta, Rev. Cancer 1877 (3) (2022) 188729, https://doi.org/10.1016/j.bbcan.2022.188729.

[13] H. Zhou, L. Zhu, J. Song, G. Wang, P. Li, W. Li, P. Luo, X. Sun, J. Wu, Y. Liu, S. Zhu, Y. Zhang, Liquid biopsy at the frontier of detection, prognosis and progression monitoring in colorectal cancer, Mol. Cancer 21 (1) (2022) 86, https://doi.org/10.1186/s12943-022-01556-2.

[14] M. Fakih, J. Sandhu, C. Wang, J. Kim, Y.J. Chen, L. Lai, K. Melstrom, A. Kaiser, Evaluation of comparative surveillance strategies of circulating tumor DNA, imaging, and carcinoembryonic antigen levels in patients with resected colorectal cancer, JAMA 5 (3) (2022) e221093, https://doi.org/10.1001/jamanetworkopen.2022.1093.

[15] W. Jue, L. Lulu, Z. Yan, S. Gu, Expression levels and diagnostic value of serum GDNF, CEA and CA199 in patients with colorectal carcinoma, J. Med. Biochem. 43 (2) (2024) 250–256, https://doi.org/10.5937/jomb0-44745.

[16] X. Su, Z. Shan, S. Duan, Harnessing extracellular vesicles using liquid biopsy for cancer diagnosis and monitoring: highlights from AACR Annual Meeting 2024, J. Hematol. Oncol. 17 (1) (2024) 55, https://doi.org/10.1186/s13045-024-01577-y.

[17] A. Takano, T. Fukuda, T. Shinjo, M. Iwashita, E. Matsuzaki, K. Yamamichi, M. Takeshita, T. Sanui, F. Nishimura, Angiopoietin-like protein 2 is a positive regulator of osteoblast differentiation, Metabolism 69 (2017) 157–170, https://doi.org/10.1016/j.metabol.2017.01.006.

[18] Y. Doi, T. Ninomiya, Y. Hirakawa, O. Takahashi, N. Mukai, J. Hata, M. Iwase, T. Kitazono, Y. Oike, Y. Kiyohara, Angiopoietin-like protein 2 and risk of type 2 diabetes in a general Japanese population: the Hisayama study, Diabetes Care 36 (1) (2012) 98–100, https://doi.org/10.2337/dc12-0166%JDiabetesCare.

[19] T. Usui, T. Ninomiya, M. Nagata, O. Takahashi, Y. Doi, J. Hata, M. Fukuhara, T. Kitazono, Y. Oike, Y. Kiyohara, Angiopoietin-like protein 2 is associated with chronic kidney disease in a general Japanese population: the Hisayama Study, Circ. J. 77 (9) (2013) 2311–2317, https://doi.org/10.1253/circj.cj-12-1548.

[20] M. Endo, M. Nakano, T. Kadomatsu, S. Fukuhara, H. Kuroda, S. Mikami, T. Hato, J. Aoi, H. Horiguchi, K. Miyata, H. Odagiri, T. Masuda, M. Harada, H. Horio, T. Hishima, H. Nomori, T. Ito, Y. Yamamoto, T. Minami, S. Okada, T. Takahashi, N. Mochizuki, H. Iwase, Y. Oike, Tumor cell-derived angiopoietin-like protein ANGPTL2 is a critical driver of metastasis, Cancer Res. 72 (7) (2012) 1784–1794, https://doi.org/10.1158/0008-5472.Can-11-3878.

[21] Y. Toiyama, K. Tanaka, T. Kitajima, T. Shimura, M. Kawamura, A. Kawamoto, Y. Okugawa, S. Saigusa, J. Hiro, Y. Inoue, Y. Mohri, A. Goel, M. Kusunoki, Elevated serum angiopoietin-like protein 2 correlates with the metastatic properties of colorectal cancer: a serum biomarker for early diagnosis and recurrence, Clin. Cancer Res. 20 (23) (2014) 6175–6186, https://doi.org/10.1158/1078-0432.Ccr-14-0007.

[22] Y. Fan, M. Lv, Y. Xue, J. Li, E. Wang, In situ fluorogenic reaction generated via ascorbic acid for the construction of universal sensing platform, Anal. Chem. 93 (17) (2021) 6873–6880, https://doi.org/10.1021/acs.analchem.1c00967.

[23] Y. Hu, Z. Wang, L. Liu, J. Zhu, D. Zhang, M. Xu, Y. Zhang, F. Xu, Y. Chen, Mass spectrometry-based chemical mapping and profiling toward molecular understanding of diseases in precision medicine, Chem. Sci. 12 (23) (2021) 7993–8009, https://doi.org/10.1039/d1sc00271f.

[24] F. Wu, H. Wang, J. Lv, X. Shi, L. Wu, X. Niu, Colorimetric sensor array based on Au_2Pt nanozymes for antioxidant nutrition quality evaluation in food, Biosens. Bioelectron. 236 (2023) 115417, https://doi.org/10.1016/j.bios.2023.15417.

[25] Y. Xiong, Y. Leng, X. Li, X. Huang, Y. Xiong, Emerging strategies to enhance the sensitivity of competitive ELISA for detection of chemical contaminants in food samples, Trends Anal. Chem. 126 (2020) 115861, https://doi.org/10.1016/j.trac.2020.115861.

[26] G. Weng, Z. Liu, J. Chen, F. Wang, Y. Pan, Y. Zhang, Enhancing the mass spectrometry sensitivity for oligonucleotide detection by organic vapor assisted electrospray, Anal. Chem. 89 (19) (2017) 10256–10263, https://doi.org/10.1021/acs.analchem.7b01695.

[27] L. Wu, J. Lin, H. Wang, K. Pan, X. Shi, X. Niu, Portable colorimetric sensor array based on a porous single-atom Fe nanozyme with different surface sites for identifying artificially ripened fruits, Adv. Funct. Mater. 35 (2) (2025) 2413154, https://doi.org/10.1002/adfm.202413154.

[28] K. Li, S. Luo, S. Guan, B. Situ, Y. Wu, Z. Ou, M. Tao, L. Zheng, Z. Cai, Tetrahedral framework nucleic acids linked CRISPR/Cas13a signal amplification system for rare tumor cell detection, Talanta 1 (247) (2022) 123531, https://doi.org/10.1016/j.talanta.2022.123531.

[29] J. Zhang, J. Xiang, L. Liao, B. Jiang, R. Yuan, Y. Xiang, Proximity binding-initiated DNA walker and CRISPR/Cas12a reaction for dual signal amplification detection of thrombin, Talanta 256 (2023) 124286, https://doi.org/10.1016/j.talanta.2023.124286.

[30] J.T. Zwerus, N.F. Berghuis, J.M. Jacques, R. Mars-Groenendijk, R.W. Busker, A. Paauw, A.L. de Jong, H.C. van Leeuwen, A TdT-driven amplification loop increases CRISPR-Cas12a DNA detection levels, Biosens. Bioelectron. 261 (2024) 116464, https://doi.org/10.1016/j.bios.2024.116464.

[31] S. Ding, Y. Wei, G. Chen, F. Du, X. Cui, X. Huang, Y. Yuan, J. Dong, Z. Tang, Detection of cancer marker flap endonuclease 1 using one-pot transcription-powered clustered regularly interspaced short palindromic repeat/Cas12a signal expansion, Anal. Chem. 94 (39) (2022) 13549–13555, https://doi.org/10.1021/acs.analchem.2c03054.

[32] J. Shi, C. Lei, W. Fan, Y. Sun, C, Liu Ultrasensitive protein and exosome analysis based on a rolling circle amplification assisted-CRISPR/Cas12a strategy, Talanta 273 (2024) 125906, https://doi.org/10.1016/j.talanta.2024.125906.

[33] Y. Xiong, J. Zhang, Z. Yang, Q. Mou, Y. Ma, Y. Xiong, Y. Lu, Functional DNA regulated CRISPR-Cas12a sensors for point-of-care diagnostics of non-nucleic-acid targets, J. Am. Chem. Soc. 142 (1) (2020) 207–213, https://doi.org/10.1021/jacs.9b09211.

[34] S. Peng, Z. Tan, S. Chen, C. Lei, Z. Nie, Integrating CRISPR-Cas12a with a DNA circuit as a generic sensing platform for amplified detection of microRNA, Chem. Sci. 11 (28) (2020) 7362–7368, https://doi.org/10.1039/d0sc03084h.

[35] W. Chen, S. Wu, G. Li, X. Duan, X. Sun, S. Li, Y. Zhao, D. Gu, G. Zeng, H. Liu, Accurate diagnosis of prostate cancer with CRISPR-based nucleic acid test strip by simultaneously identifying PCA3 and KLK3 genes, Biosens. Bioelectron. 220 (2023) 114854, https://doi.org/10.1016/j.bios.2022.114854.

[36] M. Sohail, L. Qin, S. Li, Y. Chen, M.H. Zaman, X. Zhang, B. Li, H. Huang, Molecular reporters for CRISPR/Cas: from design principles to engineering for bioanalytical and diagnostic applications, TrAC, Trends Anal. Chem. 149 (2022) 116539, https://doi.org/10.1016/j.trac.2022.116539.

[37] X. Cheng, Y. Li, J. Kou, D. Liao, W. Zhang, L. Yin, S. Man, L. Ma, Novel non-nucleic acid targets detection strategies based on CRISPR/Cas toolboxes: a review, Biosens. Bioelectron. 215 (2022) 114559, https://doi.org/10.1016/j.bios.2022.114559.

[38] T. Yan, K. Yang, C. Chen, Z. Zhou, P. Shen, Y. Jia, Y. Xue, Z. Zhang, X. Shen, X. Han, Synergistic photothermal cancer immunotherapy by Cas9 ribonucleoprotein-based copper sulfide nanotherapeutic platform targeting PTPN2, Biomaterials 279 (2021) 121233, https://doi.org/10.1016/j.biomaterials.2021.121233.

[39] J. Zhao, L. Yang, Y. Dai, Y. Tang, X. Gong, D. Du, Y. Cao, Peptide-templated multifunctional nanoprobe for feasible electrochemical assay of intracellular kinase, Biosens. Bioelectron. 119 (2018) 42–47, https://doi.org/10.1016/j.bios.2018.07.063.

[40] T.T. Tsai, C.A. Chen, N. Yi-Ju Ho, S. Yang, C.F. Chen, Fluorescent double-stranded DNA-templated copper nanoprobes for rapid diagnosis of tuberculosis, ACS Sens. 4 (11) (2019) 2885–2892, https://doi.org/10.1021/acssensors.9b01163.

[41] M. Huang, E. Xiong, Y. Wang, M. Hu, H. Yue, T. Tian, D. Zhu, H. Liu, X. Zhou, Fast microwave heating-based one-step synthesis of DNA and RNA modified gold nanoparticles, Nat. Commun. 13 (1) (2022) 968, https://doi.org/10.1038/s41467-022-28627-8.